Feasibility Study of a Low-power Applied-field MPD Arcjet

Tetsuaki NAKANO, and Atsushi ISHIYAMA
Waseda University
3-4-1 Ohkubo, Shinjuku, Tokyo, Japan
+81-3-5286-3187
(E-mail:nakano@ep.isas.ac.jp)

Yukio SHIMIZU and Kyoichiro TOKI
Institute of Space and Astronautical Science
3-1-1 Yoshinodai, Sagamihara, Kanagawa 229-8510, Japan

IEPC-03-92

A Research has been initiated on a 1kW-class applied-field MPD arcjet, including evaluation of thruster performance as well as its feasibility. As the result 1kW-class stady-state MPD arcjet was proved to be attainable. At the present, it was found that stable operation is achieved with Ar, Ne and He propellant at a mass flow rate down to 100 sccm, under an applied magnetic field of 0.20 Tesla, resulting in only 25 Amperes of discharge current. This thruster gave a thrust efficiency of 8.5 % and a specific impulse of 1600 sec for Ar, 1100sec for Ne and 2200 for He.

Introduction

Self-field MPD arcjets, of electromagnetic thrusters, are able to attain both high specific impulse and high thrust density. However, in order to generate high thrust efficiency, very large input powers (larger than 100kW) must be supplied, since most of the thrust is generated by a large arc discharge current (greater than 2kA) and its self-induced magnetic field. In fact, operating such device steadily on an orbiting satellite is very difficult, since at present solar arrays equivalent to that high power become very huge.

In this respect, instead of attempting to reduce the arc discharge current and the self-induced magnetic field inside the thruster. The concept of having an applied-field MPD thrusters with solenoidal coils in order to provide a desirable magnetic field inside discharge chamber for raising the Lorenz force level, has been considered in a few organizations. One of these research efforts was conducted by Sasoh and Arakawa at University of Tokyo[1] with a 10kW-class applied-field MPD thruster, aiming high performance. In this case, in spite of its low power level, comparatively high thruster performance was reported. Then we have started to research about a 1kW-class applied-field MPD arcjet which has never been attempted. The first step objectives are 1) stabilizing the arc discharge at low current and low mass flow rate range, 2) producing electromagnetic thrust and increasing specific impulse to the range which can not attain by electrothermal thrusters, 3) giving insight of the feasibility of the device.

Experimental Apparatus

The 1 kW-class steady-state MPD arcjet used in this study is shown in Fig. 1 and Fig. 2. An external magnetic field applied in the interelectrode region is provided by two solenoidal coils connected in series. A part of walls outside the coils is made of soft iron and providing magnetic circuit. Such circuit has following two roles: 1) Increasing intensity of magnetic field inside the discharge chamber, 2) Reducing interaction of the magnetic flux leakage to avoid force interaction with power lines and in practical use the spacecraft environment. The calculated magnetic flux is depicted in Fig. 3 and the variation of magnetic flux density along the centerline of the device is shown in Fig. 4. Three types of anodes were examined to evaluate the stability of arc discharge and thrust performance. The configuration of these three anodes are

Presented as Paper IEPC-03-92 at the 28th International Electric Propulsion Conference, Touluse, France, 17-21 March 2003.

converging-diverging type and having 28mmϕ and a nozzle half angle of 25°. The throat diameter is varied and the throat length is 2mm. These anodes geometry is shown in Fig. 5. The cathodes are 2% thoriated tungsten having a diameter of 5mm or 3mm with conical tip. The insulator is made of boron-nitride for high temperature parts, and a Macor ceramic for moderate temperatures.

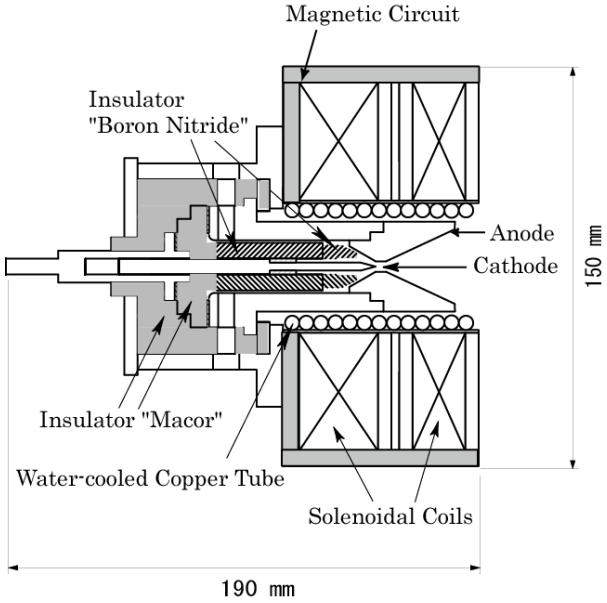

Fig.1 Cross sectional view of a 1 kW-class applied-field MPD arcjet

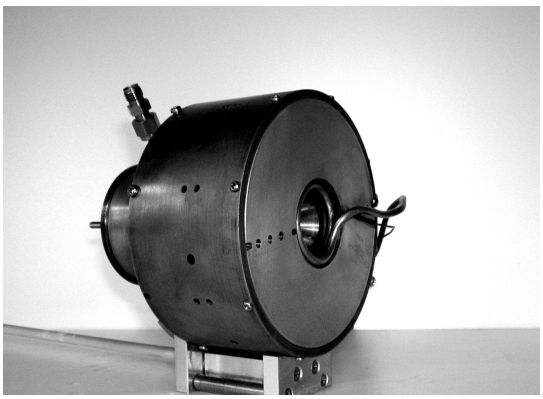

Fig .2 1kW-class applied-field MPD arcjet

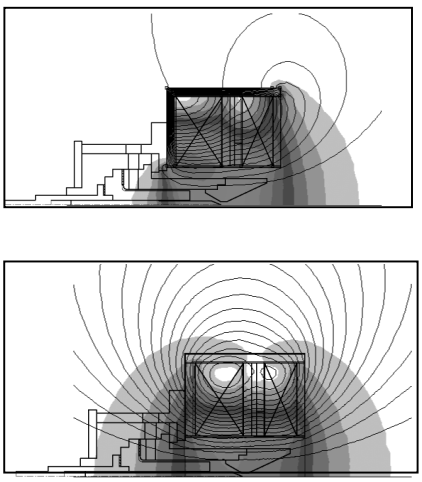

Fig.3 Calculated magnetic flux geometry (Upper: with magnetic circuit, Lower: no-magnetic circuit)

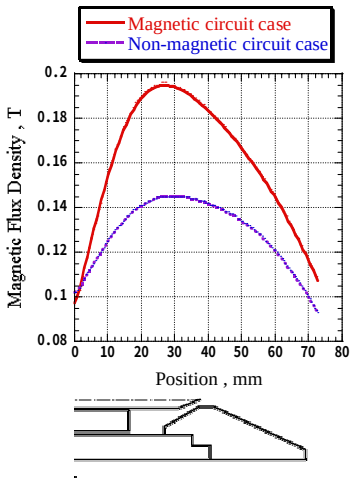

Fig.4 An Example of magnetic flux density distribution along the centerline (Current density of coils: 6×10^{6} [A/m^2])

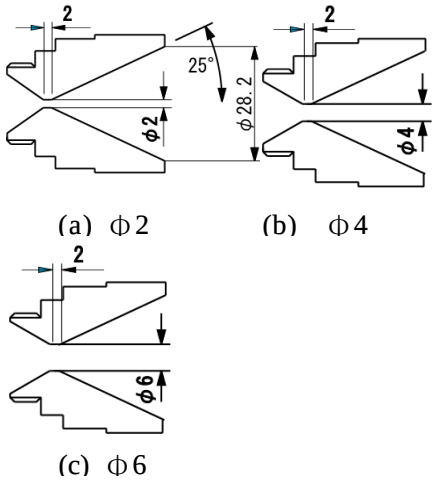

Fig.5 Anode geometries

A schematic diagram of experimental apparatus is shown in Fig. 6. The MPD arcjet was placed in a vacuum chamber with 0.8mϕ and 2m long and the background pressure during operation was kept under 5×10^{-4} Torr. The discharge power was supplied by a switching-regulator type DC power source of constant current, equipped with a high-voltage pulse for ignition. The coil current for applied-field was supplied by another DC power source of series regulator type. A water cooling was applied only into the inner wall of solenoidal coils, so the discharge electrodes were radiatively cooled.

Ar, Ne and He gas were used as the propellant and the supply system was bifurcated by different flow rates. One line can regulate higher mass flow rate (over 30mg/s, Ar) just in the start-up phase of arc discharge. The other line controls smaller propellant flow rates (under 5mg/s, Ar) at steady-state operation.

The discharge voltage was measured by a divided resistor consisting of the 3.9MΩ and the 0.1MΩ resistors connected in parallel to the electrode gap. The discharge current was measured by a Hall-effect current sensor.

The thrust measurement was conducted by gradient method on the slope (Fig. 7). This system is composed of a slope, bearings and a load cell. The load cell has a capacity of 1N and can detect as low as 0.3mN. A water-cooled copper tube was fixed on the side wall of the load cell in order to prevent the zero drift caused by joule heating of internal resistance. The electromagnetic interaction force exerted on power lines for arc discharge could be eliminated down to the negligible level by reducing magnetic flux leakage to the power lines.

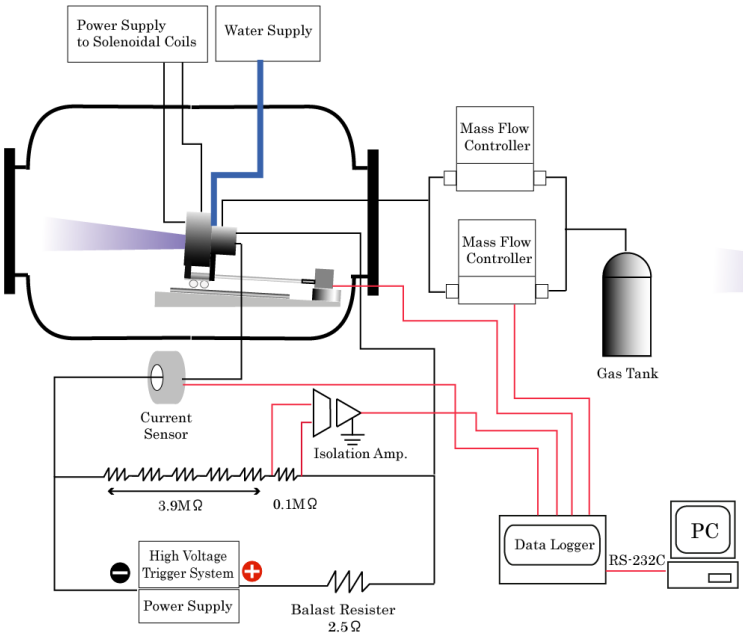

Fig.6 Experimental set-up for 1kW steady-state MPD arcjet

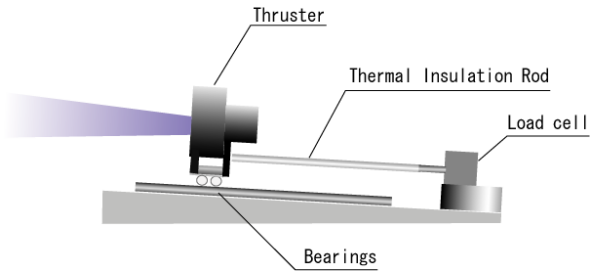

Fig. 7 Thrust measurement system

Experimental Result

Arc Discharge Stability

The operating condition of this device is shown in Table 1. In our previous work[2] on this device, in order to generate effective electromagnetic thrust, we paid every effort on the reduction of mass flow rate. It must be drastically reduced to the lower range than the typical electrothermal thruster. However, as the mass flow rate and the discharge current decrease, the discharge becomes unstable. We investigated the arc discharge stability by varying electrodes geometry, mass flow rate and applied magnetic field intensity and established methodology of increasing arc discharge stability.

First, we examined the arc discharge stability by using cathode with 5mmϕ and three types anodes shown in Fig. 5(a)(b)(c). The cathode tip location is fixed at the upstream inlet of throat (Anode-Cathode gap is 0). These electrodes configurations are shown in Fig. 8. Table 2 shows the results of arc discharge stability. By using anode with smallest throat diameter (ϕ2) arc discharge is quite stable, however, as the anode throat diameter increases, the discharge becomes unstable.

For lower mass flow rates, electron emitted from cathode surface tends to flow along the magnetic field line, since the expected electron collision frequency with heavy particles is relatively low. Thus the arc discharge cannot be stabilized when discharge current path to the throat is perpendicular to magnetic field. As throat diameter of anode increases, current path approaches perpendicular to magnetic field and results in decrease of arc discharge stability.

In order to increase the arc discharge stability even in the anode with larger throat diameters, following

two configurations were incorporated. 1) Moving cathode tip to the upstream direction as throat diameter increases. 2) Changing cathode's diameter from 5mm to 3mm.

By recessing the cathode tip, discharge current path tends to be parallel to the magnetic field lines and give rise to stable arc discharge. And by replacing to a smaller diameter cathode, the spot fluctuation of arc discharge is suppressed since the electron emission point is attached at the center of cathode tip, and enhancing the thermionic emission to stabilize the rigid arc.

Improved electrodes geometry and placements are shown in Fig. 9, and Table 3 shows the arc discharge stability with these improved configurations. As shown in Table 3, arc discharge was more extensively stabilized by improving electrode configurations.

Table 1: Operating condition

Discharge current , A	8 - 36
Applied magnetic field intensity , T	0.10 - 0.20
Propellant	Ar, Ne, He
Mass flow rate , mg/s	0.5 - 5 (Ar) 1.5 (Ne) 0.2 - 0.5 (He)

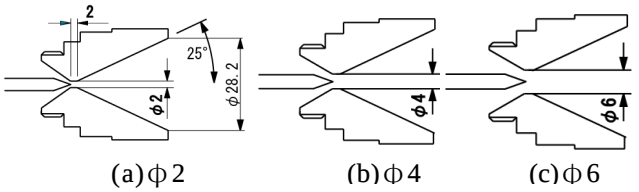

(a)φ2 (b)φ4 (c)φ6

Fig.8 Electrode configuration

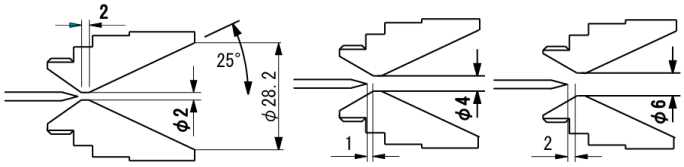

(a)φ2 (b)φ4 (c)φ6

Fig.9 Improved electrode configuration

Table 2: Arc discharge stability evaluation with electrodes shown in Fig.8 (discharge current: 21A)

		Mass flow rate (Ar) mg/s		
	B , T	1	3	5
φ2	0.10	**stable**	**stable**	**stable**
	0.15	**stable**	**stable**	**stable**
φ4	0.10	No discharge	**Unstable**	**stable**
	0.15	No discharge	**Unstable**	**stable**
φ6	0.10	No discharge	No discharge	No discharge
	0.15	No discharge	No discharge	**Unstable**

Table 3: Arc discharge stability evaluation with electrodes shown in Fig.9 (discharge current: 25A)

		Mass flow rate (Ar) mg/s		
	B , T	1	3	5
φ2	0.10	**stable**	**stable**	**stable**
	0.15	**stable**	**stable**	**stable**
φ4	0.10	**stable**	**stable**	**stable**
	0.15	**stable**	**stable**	**stable**
φ6	0.10	**Unstable**	**stable**	**stable**
	0.15	**Unstable**	**stable**	**stable**

Effect of Anode Geometry on Thrust

Thrust was measured for varying electrodes shown in Fig.9. Fig.10-(a) shows thrust vs. applied magnetic field intensity characteristics and Fig.10-(b) shows discharge voltage vs. applied magnetic field intensity characteristics. The anode with the smallest throat diameter(φ2) has advantage for the stabilization of arc discharge, however, the performance with this anode(φ2) is the worst among these three anodes. Both the thrust and the discharge voltage are insensitive to the applied magnetic field. By changing the anodes toward larger throat diameter(φ4 and φ6) the performance is dramatically improved and thrust and discharge voltage is proportional to applied magnetic field intensity.

Fig.11-(a) shows thrust vs. discharge current and Fig. 11-(b) shows discharge voltage vs. current characteristics. By increasing discharge current, nevertheless the performance with anode(φ2) was not

improved, the performances with anodes having larger throat diameter (ϕ4 and ϕ6) are improved. V-I curves have negative characteristics in anode(ϕ2) and anode(ϕ4) case, however in anode(ϕ6) case discharge voltage tends to increase with increasing discharge current.

Exhaust Plume

Exhaust plume photographs are arranged in the order of specific impulse in Fig.12. These photographs show a correlation between exhaust plume feature and specific impulse. As the plume pinched along the central axis, so-called "cathode jet" is observed clearly, higher specific impulse is obtained. By reducing mass flow rate or using anode with larger throat diameter, brighter cathode jet tends to be concentrated.

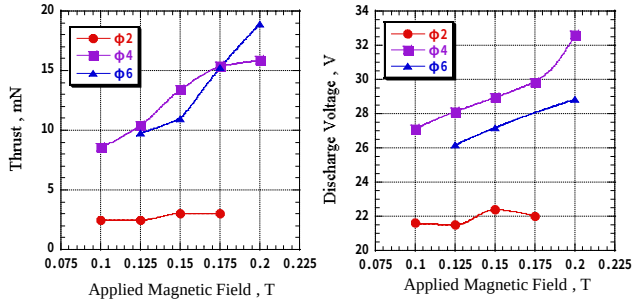

(a) F-B characteristics (b) V-B characteristics

Fig.10 Dependence on applied field intensity (Discharge current: 25A, Mass flow rate: 3mg/s Ar)

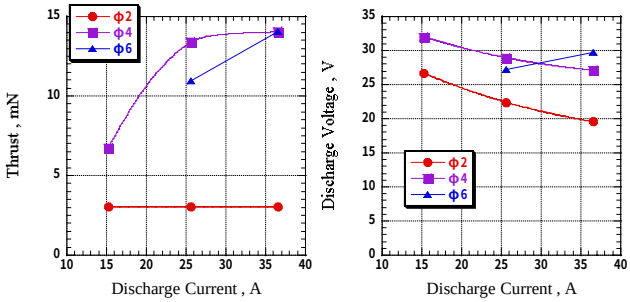

(a) F-I characteristics (b) V-I characteristics

Fig.11 Dependence on discharge current (Applied magnetic field: 0.15T, Mass flow rate: 3mg/s Ar)

(a) Specific impulse: 450 sec
Discharge current: 25A
Applied field: 0.15T
Mass flow rate: 3mg/s (Ar)
Anode: ϕ4

(b) Specific impulse: 300 sec
Discharge current: 25A
Applied field: 0.15T
Mass flow rate: 5mg/s (Ar)
Anode: ϕ4

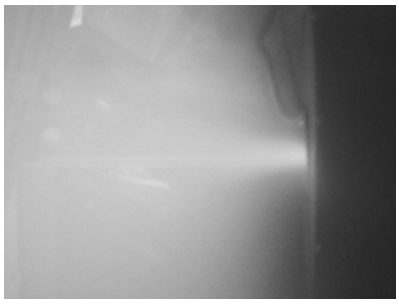

(c) Specific impulse: 100 sec
Discharge current: 25A
Applied field: 0.15T
Mass flow rate: 3mg/s (Ar)
Anode: ϕ2

Fig.12 Exhaust plume varation

Effect of Background Pressure on Thrust

Sovie and Connolly[3] have reported that thrust measurement is affected by entrainment of ambient gas from the exhaust plume when the background pressure in the vacuum chamber is high. In a typical high current MPD arcjet this kind of illusive thrust is observed at insufficiently low background pressure. They pointed out that in order to ignore this effect thrust measurement must be conducted at background pressures bellow 2×10^{-4} Torr.

Figure. 13 shows the effect of ambient gas on thrust value. In case of this study, thrust is largely decreased at higher background pressure and this trend suggests no possible entrainment phenomenon. Operations at lower background pressure provide favorable possibility of more improved thrust performance in our case.

Thruster Performance

Thruster performance obtained in the experiment is summarized in Fig. 14 and Fig. 15. Here, the specific impulse I_{sp} and thrust efficiency η are given by, respectively,

$$I_{sp} = \frac{F}{\dot{m}g}$$

$$\eta = \frac{F^2}{2\dot{m}P_{arc}}$$

Here, the electrical power supplied to the solenoidal coils is not taken into account in the calculation of the input power.

Figure. 14 shows thruster performance by varying electrode configuration with Ar propellant. In the anode(ϕ2) for Ar propellant case, thrust efficiency at almost all the operating points do not exceed 1%. In the anode(ϕ4) and the anode(ϕ6) case, thruster performance was improved. The highest specific impulse for Ar propellant is 1600sec obtained at applied magnetic field of 0.20T, discharge current of 25A , mass flow rate of 1mg/s with anode(ϕ6), however the discharge voltage oscillation occurred at this operating point. The highest thrust-to-power ratio of 29mN/kW was obtained.

Figure. 15 shows thruster performance by varying propellant with the anode(ϕ4). In this operating condition, the highest specific impulse is 550sec for Ar, 1100sec for Ne and 2200sec for He. On the contrary, thrust-to-power ratio for Ar propellant of 21mN/kW exceeded Ne propellant case of 12 mN/kW and He popellant case of 7mN/kW.

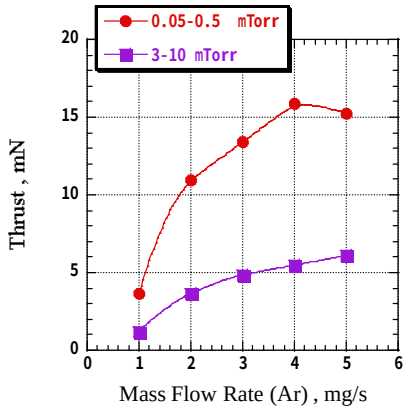

Fig. 13 Effect of background pressure on thrust (Discharge current: 25A, Applied magnetic field: 0.15T, Anode: ϕ4)

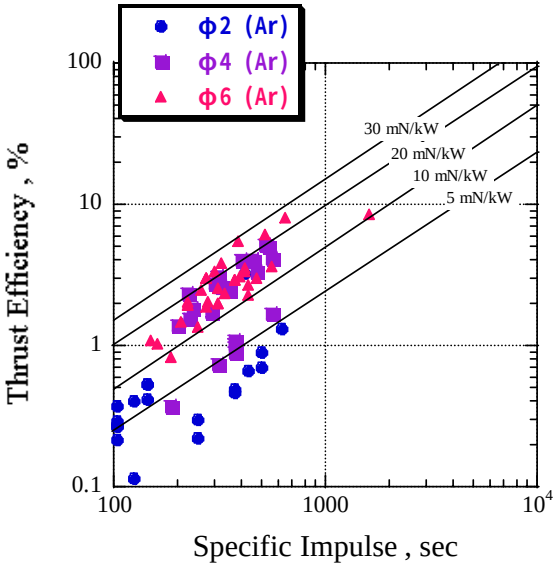

Fig. 14 Thruster performance of 1kW-class applied-field MPD arcjet by varying electrode configuration

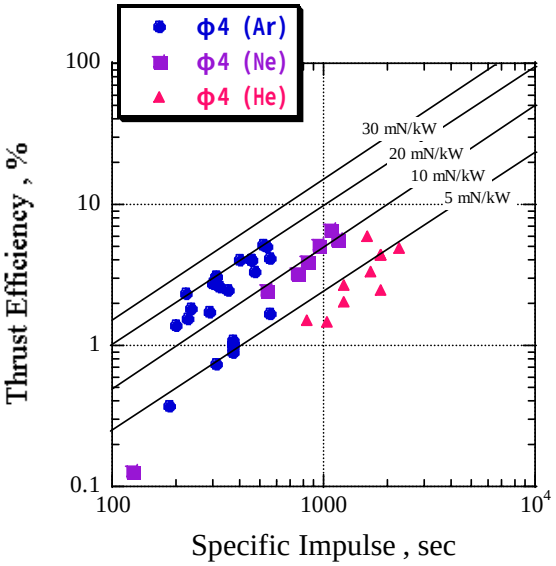

Fig. 15 Thruster performance of 1kW-class applied-field MPD arcjet by varying propellant

Acceleration Mechanisms

Considering the acceleration mechanism of this thruster, it is worthwhile noting that there are two approaches to explain the acceleration mechanisms in applied-field MPD thrusters. These are briefly described below[4]

Generalized Hall acceleration: An axial electromagnetic force is produced by the interaction between the azimuthal induced current and the radial magnetic field. The azimuthal current is induced due to not only the E×B drift of electron (Hall current) but also the diamagnetic effect.(Fig. 16)

Swirl acceleration: An azimuthal electromagnetic force is produced by the radial supplied discharge current and the axial applied magnetic field ($j_r B_z$). This azimuthal force causes the swirl motion of the propellant plasma flow, resulting in swirl kinetic energy gain. The swirl kinetic energy can be converted into axial kinetic energy both through the solid nozzle of the thruster, and the magnetic nozzle formed by the applied magnetic field (conservation of magnetic moment)(Fig. 17).

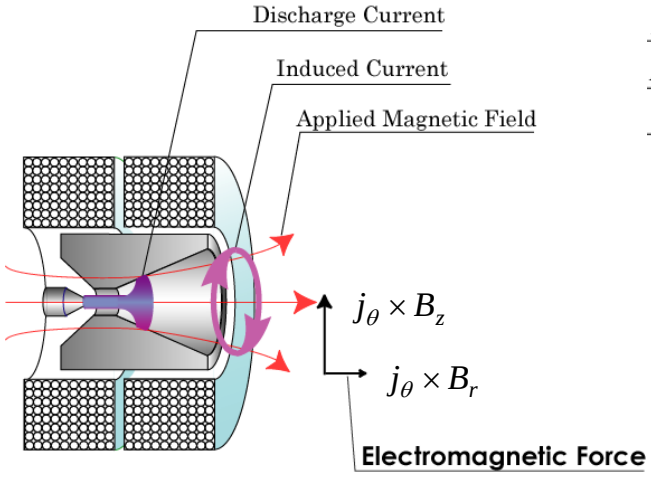

Fig.16 Generalized Hall acceleration

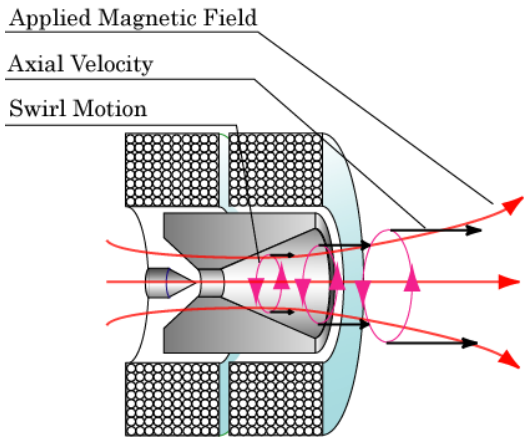

Fig. 17 Swirl acceleration

For our experiment, judging from the pinched exhaust plume caused by the Lorentz force between the azimuthal induced current and the axial magnetic field, it seems that main acceleration mechanism is generalized Hall acceleration and azimuthal induced current play a very important role on the thrust production.

If azimuthal current is mainly induced by electron E×B drift, the acceleration mechanism partly becomes the same as the Hall thrusters. However, by increasing applied magnetic field, E×B drift velocity of electron decreases and thus discharge voltage should not increase. In Fig.10-(a), increase of magnetic field intensity result in increase of thrust and discharge voltage. This result indicates that dominant mechanism which effects on azimuthal motion of plasma is not E×B drift.

An azimuthal electromagnetic force produced by the radial discharge current and the axial applied magnetic field causes the swirl motion of the plasma flow and the discharge voltage is increased. Then mean free time is long enough for electrons to complete cyclotron motion, only ions collide with the anode surface because of its large Larmor radius. By causing azimuthal velocity slip between ions and electrons, azimutal electron current is induced. Hence there is a possibility that the induced azimuthal current mechanism of this thruster has a similarity with that of typical Hall thrusters. On the other hand in the downstream, the azimuthally induced current produces axial thrust by interaction with radially expanding magnetic fields lines. This is truly an MPD $j_\theta \times B_r$ acceleration of plasma and totally different from that of Hall thruster.

In order to induce azimuthal current, plasma density is required to be relatively low but larger than that required for typical Hall thrusters. Hence this thruster is expected to be able to operate at larger thrust density compared with Hall thrusters.

Our future studies will be focused on clarifying the mechanism of thrust and azimuthal current production by means of plasma diagnosis.

CONCLUSIONS

A 1kw-class steady-state applied-field MPD arcjet was designed and tested for a variety of operational conditions and thrust measurement is conducted by gradient method on the slope applying load cell.

Stabilization of the arc discharge was eventually realized by using an anode with smaller throat diameter and by shifting the position of cathode tip and using a cathode with smaller diameter, arc discharge stability is dramatically improved.

Better thruster performance was observed by using anode with larger throat diameter, and the specific impulse of 1600sec for Ar, 1100sec for Ne and 2200sec for He are obtained.

Even in the electrical input power of 1kW, we have confirmed that the electromagnetic thrust turns out to be dominant judging from the delivered I_{sp} and it is concluded that a 1kW-class steady-state applied-field MPD arcjet is reached in this study.

REFERENCES

[1] Sasoh, A., "Thrust Performance and Acceleration Mechanisms of Steady-State Applied-Field MPD Arcjets," Ph D Thesis, University of Tokyo, March 1989.

[2] Toki, K., and Shimizu, Y., " Study of Low-Power MPD propulsion for Future High-Power trend," Proceedings of the 38th Joint Propulsion Conference, AIAA 2002-4115, Indianapolis, Indiana, USA., July. 2002.

[3] Sovie, R. J., and Connoly, D. J., "Effect of Background Pressure on Magnetoplasmadynamic Thruster Operation, " Journal of Spacecraft and Rockets, Vol.7, March 1970, pp.255-258.

[4] Sasoh, A., and Arakawa, Y., "Thrust Formula for an Applied Field MPD Thruster from Energy Conservation Equation, " Proceedings of the 22nd International Electric Propulsion Conference, IEPC91-062, Viareggio, Italy, Oct. 1991.

[5] Toki, K., and Shimizu, Y., "A Study of Low-Power MPD Arcjets for Future High-Power Evolution," Proceedings of the 27th International Electric Propulsion Conference, IEPC-01-120, Pasadena, California, USA., Oct. 2001.

[6] Kruelle, G., Auweter-Kuruz, M. and Sasoh, A., "Technology and Application Aspects of Applied Field Magnetoplasmadynamic Propulsion," Journal of Propulsion and Power, Vol. 14, No.5, Sept.-Oct. 1998, pp. 754-763.